

Evolution of Li, Be and B in the Galaxy

Giada Valle and Federico Ferrini

*Dipartimento di Fisica
Università di Pisa
Piazza Torricelli 2
I-56100 Pisa, Italy*

giada,federico@astr2pi.difi.unipi.it

Daniele Galli

*Osservatorio Astrofisico di Arcetri
Largo Enrico Fermi 5
I-50125 Firenze, Italy*

galli@arcetri.astro.it

Steven N. Shore

*Department of Physics and Astronomy
Indiana University South Bend
1700 Mishawaka Ave, South Bend
IN 46634-7111 USA*

and

*Osservatorio Astrofisico di Arcetri
Largo Enrico Fermi 5
I-50125 Firenze, Italy*

sshore@paladin.iusb.edu

ABSTRACT

In this paper we study the production of Li, Be and B nuclei by Galactic cosmic ray spallation processes. We include three kinds of processes: (*i*) spallation by light cosmic rays impinging on interstellar CNO nuclei (*direct* processes); (*ii*) spallation by CNO cosmic ray nuclei impinging on interstellar *p* and ^4He (*inverse* processes); and (*iii*) α - α *fusion* reactions. The latter dominate the production of $^6,^7\text{Li}$. We calculate production rates for a closed-box Galactic model, verifying the quadratic dependence of the Be and B abundances for low values of *Z*. These

are quite general results and are known to disagree with observations. We then show that the multi-zone multi-population model we used previously for other aspects of Galactic evolution produces quite good agreement with the *linear* trend observed at low metallicities *without fine tuning*. We argue that reported discrepancies between theory and observations do not represent a nucleosynthetic problem, but instead are the consequences of inaccurate treatments of Galactic evolution.

Subject headings: Galaxy: evolution — cosmic rays — Galaxy: abundances

1. Introduction

The formation of the lightest elements beyond helium (${}^6,{}^7\text{Li}$, ${}^9\text{Be}$, ${}^{10,11}\text{B}$, hereafter LiBeB) has persisted as a major problem for nucleosynthesis for many decades. The history is well known and we will not review it here (see Spite & Pallavicini 1995; Prantzos, Tosi, & von Steiger 1998; Ramaty et al. 1999; Fields & Olive 1999a,b; Vangioni-Flam et al. 2000; Fields et al. 2000). Recent observational advances have again brought these elements to center stage as data become available for ancient, extremely low metallicity stars in the Galactic halo and contemporary, interstellar diffuse gas.

Several separate issues must be addressed regarding the time development of light element abundances in the Galaxy. The *Spite plateau* appears to be the floor for ${}^7\text{Li}$ and *may* represent its primordial value. Both isotopes of Li are easily destroyed in stellar interiors so the likely source for the greater than primordial abundances must be extra-stellar. For this reason spallation reactions by Galactic cosmic rays (GCR) interacting with nuclei in the diffuse interstellar medium (ISM) have been implicated as avenues for light element Galactic synthesis. Recent observations tax the simple spallation models that have p and α cosmic rays reacting with stationary interstellar heavy nuclei. As we will show, because the heavy nuclei and massive cosmic rays come from the same ultimate source – stars and their supernova remnants – the abundance of ${}^6\text{Li}$, Be, and B should all scale as Z^2 . This prediction is severely at odds with the observational data at low metallicity (Duncan et al. 1998; Boesgaard et al. 1999). This picture can be modified in several ways. Inverting the reasoning, Prantzos et al. (1993) proposed that a change in the slope and lower energy cutoff of GCRs over Galactic history can enhance the production of the light nuclei and produce an almost linear dependence on Z . Duncan et al. (1997) argued that including fusion and inverse reactions, those for which the high energy particles are accelerated CNO spalling stationary hydrogen and helium in the ISM, will produce the right metallicity scaling for even ${}^7\text{Li}$. Fields & Olive (1999a) and Fields et al. (2000) have shown that in a closed box

model the early evolution of LiBeB can be explained using the standard rates provided the O/Fe ratio is allowed to float with time, increasing at low Z . These calculations were all performed assuming only single galactic zones, albeit including simple infall prescriptions.

Our aim in this paper is to contrast the predictions of two broad classes of schemes for treating Galactic chemical and population evolution: simple closed box models, and more developed multi-zone, multi-population models. We will show that many of the theoretical puzzles noted in the literature are simply paradoxes arising from assumptions in the closed one-zone models. These cannot be repaired by more accurate prescriptions of the yields and delays due to stellar evolution. They are endemic to the basic feature of the models since the system maintains constant mass without feedback and the star formation is a monotonically decreasing function of time according to a Schmidt-type power law in gas density (or surface density).

Once the nuclear reactions involved in the production of LiBeB nuclei are established, a Galactic evolution model is needed to compute the ISM abundances evolution and the SN rates. Two extreme choices are possible: the simple closed-box model (Tinsley 1980), or a more complex nonlinear scheme, that gives satisfactory answers to other aspects of Galactic evolution (Ferrini 1991; Ferrini et al. 1992; Pardi et al. 1995). A comparison between the two is useful to fix the limits of influence of the hypotheses for the GCR: the observational situation of LiBeB reflects simply a nuclear problem of GCR interactions with ISM, and hence depends exclusively on knowledge about their interactions.

2. Cosmic-ray nucleosynthesis

In this section we consider the nucleosynthesis scenario of spallation reactions of GCR on ISM nuclei for the production of LiBeB nuclei. Among all nuclear reactions, there are two main production channels of light elements:

(i) *direct processes*, i.e. interactions of a p or an α particle of GCR with C,N,O nuclei of the ISM, hereafter represented by $p, \alpha + \text{C,N,O} \rightarrow \text{LiBeB}$;

(ii) *inverse processes*, i.e. interactions of C,N,O nuclei of GCR with a p or an α particle of the ISM, hereafter represented by $\text{C,N,O} + p, \alpha \rightarrow \text{LiBeB}$.

For Li, *fusion reactions* must also be considered, i.e. interactions of α particles of GCR with α particles of ISM (hereafter represented by $\alpha + \alpha \rightarrow {}^6,7\text{Li}$).

The production rate of the light element ℓ (with $\ell = \text{LiBeB}$) at time t , resulting from the spallation process $i + j \rightarrow \ell$, is the convolution of the flux $\Phi_i(E_i, t)$ of the GCR projectile

nuclei i with the numerical abundance of ISM target x_j^{ISM} weighted by the spallation cross section $\sigma_{i,j \rightarrow \ell}(E_i)$,

$$r_{i,j \rightarrow \ell}(t) = x_j^{\text{ISM}}(t) \int_{E_T}^{\infty} \Phi_i(E_i, t) \sigma_{i,j \rightarrow \ell}(E_i) S_{i,j \rightarrow \ell}(E_i) dE_i, \quad (1)$$

where E_T is the threshold energy of the reaction.

We assume that only a fraction $S_{i,j \rightarrow \ell}(E_i)$ of newly produced light elements is thermalized and incorporated in the ISM, the remaining fraction becoming part of the GCR. The reaction products Li, Be and B have, in fact, different fates: they can escape from the interaction region if they have a sufficient energy, or suffer a progressive energy loss until becoming thermalized. The ability of the ISM to stop the light elements so synthesized determines the survival probability $S_{i,j \rightarrow \ell}(E_i)$ of various reaction products against escape from the interaction region and for their nuclear destruction that can occur during their slowing down. When the incident particles are p or α colliding with heavy nuclei, $S_{i,j \rightarrow \ell}(E_i) \simeq 1$. In the opposite case, and for α - α reactions, the trapping fractions are usually calculated in the framework of the *leaky-box* model (see *e.g.* Cesarsky 1980), and have the form

$$S_{i,j \rightarrow \ell}(E_i) = \int f(E_\ell[E_i]) \exp \left[-\frac{R_\ell(E_\ell)}{\Lambda} \right] dE_\ell, \quad (2)$$

where $f(E_\ell[E_i])$ is the distribution of energy of the product particle ℓ (depending on the energy E_i of the incident particle), $R_\ell(E_\ell)$ is the *stopping range* of the particle ℓ , and Λ is the ISM path length. Here we approximate the trapping fractions as constant, and we adopt the results by Mitler (1972), shown in Table 1, that are in agreement with the prescriptions by Meneguzzi et al. (1971) and other authors.

We assume that the GCR flux $\Phi_i(E, t)$ has a separable form,

$$\Phi_i(E, t) = x_i^{\text{GCR}}(t) \xi(t) \varphi(E), \quad (3)$$

where $\varphi(E)$ is the present-day cosmic ray flux (number of nuclei per unit energy time and area, see Sec. 2.1), $x_i^{\text{GCR}}(t)$ is the cosmic ray composition (by number), and $\xi(t)$ is a dimensionless function that modulates the intensity of the GCR (see Sec. 2.1), with $\xi = 1$ at the present epoch. Thus, eq. (1) becomes

$$r_{i,j \rightarrow \ell}(t) = x_i^{\text{GCR}}(t) x_j^{\text{ISM}}(t) \xi(t) \mathcal{P}_{i,j \rightarrow \ell} S_{i,j \rightarrow \ell}, \quad (4)$$

where we define the *production coefficients*

$$\mathcal{P}_{i,j \rightarrow \ell} = \int_{E_T}^{\infty} \varphi(E) \sigma_{i,j \rightarrow \ell}(E) dE. \quad (5)$$

The function $\xi(t)$ gives the time dependent intensity of GCR. Following the current interpretation, we assume that cosmic rays particles are accelerated by SN remnants, and therefore we set

$$\xi(t) = \frac{\psi_{\text{SN}}(t)}{\psi_{\text{SN}}(t_{\text{Gal}})}, \quad (6)$$

where ψ_{SN} is the global supernova rate (number of supernovae per unit time) and $t_{\text{Gal}} \simeq 13$ Gyr is the age of the Galaxy.

The composition of GCR varies with time according to the evolution of interstellar abundances. Thus we set $x_i^{\text{GCR}}(t) = x_i^{\text{ISM}}(t)$, where $x_i^{\text{ISM}}(t)$ ($i = p, \alpha, \text{C}, \text{N}, \text{O}$) is the abundance by number of the corresponding element in the ISM, calculated by our model of Galactic chemical evolution. Finally, the spallation cross sections $\sigma_{i,j \rightarrow \ell}(E_i)$ for all direct and inverse processes are taken from Read & Viola (1984), whereas the cross sections for α - α reactions are from Mercer et al. (2001).

2.1. The energy spectrum of GCR

A definitive, comprehensive theoretical framework is still lacking that is able to explain the origin and mechanism(s) of propagation of Galactic cosmic rays based on the interaction of relativistic charged particles with the interstellar matter. Approximate semiempirical models are widely used to describe the propagation of GCR, often treated as a diffusion process. The “leaky box” model is the most popular: a number of pointlike sources distributed throughout the Galaxy emits a flux of fast particles with a broad energy spectrum. The particles propagate diffusively within the Galaxy and have a certain probability of escaping. The homogeneity hypothesis allows a simplified treatment of the corresponding diffusion equation for the flux, and the propagation equation can be solved assuming steady state conditions. The solution depends on several factors: the energy losses by ionization, the mean free path for escape from the Galaxy, the mean free path for nuclear reactions, the assumed spectrum at the source, etc. Energy loss resulting from continuous ionization accounts also for the probability that a particle from the source or produced by nuclear reactions during the propagation of GCR can survive to become part of the flux.

In this work we adopt the propagated demodulated spectrum obtained by Ip & Axford (1985), which we approximate as

$$\varphi(E) = A(E + E_0)^{-\gamma}, \quad (7)$$

where E is in MeV, $E_0 = 750$ MeV, and $\gamma = 2.7$. For $E \gg E_0$ this spectrum becomes a simple power law in energy that allows to adopt the absolute flux normalization $A = 3.88 \times$

$10^6 \text{ cm}^{-2}\text{s}^{-1}\text{MeV}^{-1}$ obtained by Wiebel-Sooth & Biermann (1999) from data at $E = 1 \text{ TeV}$. Alternative choices are available in the literature (Gloecker & Jokipii 1967; Goldstein et al. 1970; Dodds et al. 1976; Reeves & Meyer 1978), but their agreement with this assumed spectrum is good. Our adopted spectrum also agrees well with the more recent results quoted by Webber (1998); discrepancies of around 50% are found below 100 MeV where solar wind modulation is important, but above that the general agreement is within 10%. We do not include an extended low energy tail that has been invoked in previous models, but as we will show in section 4, the full treatment for evolution does not require this. The values of $\mathcal{P}_{i,j \rightarrow \ell}$ for the reactions considered, evaluated with the GCR spectrum and nuclear cross section just described, are shown in Table 2. These production coefficients contain all the necessary nucleosynthesis information.

3. Analytic Results Models for Light Element Evolution in a Closed Box Formalism

The simplest representation of Galactic evolution is the single zone closed box scheme, also called the Simple Model (SM, see *e.g.* Tinsley 1980). It provides a useful, although limited, test bed for model assumptions and here we use it as a guide to more complete chemical evolution modeling that forms the next section. The main advantage of this closed box picture is that we can derive analytical expressions for the Li, Be and B abundances, evaluate orders of magnitude of the most significant quantities, and gain an idea of their trends. It should be kept in mind, however, that the model is severely restricted: there can be no net flow of mass through the zone, nor is there coupling with any other parts of the Galaxy.

In the SM, the Galaxy is a spatially homogeneous, isolated *closed volume* of fixed total mass M_0 . The gas mass M_g decreases with time from star formation at a rate ψ ,

$$\frac{dM_g}{dt} = -(1 - R)\psi, \quad (8)$$

where R is the average mass fraction, weighted by the initial mass function (IMF) $\phi(m)$, returned to the ISM by stars at the end of their evolution. In the following, we employ the instantaneous recycling approximation (IRA), and assume that stars process interstellar gas and replenish it on a timescale shorter than the typical large scale dynamical timescales. The rate of metal production by stars is:

$$M_g \frac{dZ}{dt} = P_Z \psi, \quad (9)$$

where Z is the metallicity and P_Z is the mass fraction of heavy elements newly produced and ejected by a stellar generation weighted by the IMF. As usual in such treatments, we make no distinction between the stellar and interstellar abundances. Here we adopt the numerical values obtained by Galli et al. (1995) from the same stellar and nucleosynthetic data adopted in the evolution model of Ferrini et al. (1992) $R = 0.21$ and $P_Z = 7.9 \times 10^{-3}$. In keeping with the restrictions of the IRA, massive stars are the principal nucleosynthetic agents and since the IMF remains unaltered with time, both R and P_Z are held constant.

In a closed system, since the total mass M_0 must remain fixed, M_g and t are conjugate variables and eqs. (8) and (9) yield

$$Z = -\frac{P_Z}{1-R} \ln \left(\frac{M_g}{M_0} \right), \quad (10)$$

with $Z(0) = 0$. Notice that we can include the effects of global mass loss through star-induced processes, i.e. winds, supernovae, etc., by inserting here a term proportional to ψ . The net effect is the same as reducing R . On the other hand, gas infall is not so easily treated. It actually violates the basic assumption of the closed box: there is a source of matter from outside the system. Thus M_g and Z are *explicit* functions of time and must be found numerically.

Light elements are mainly destroyed in stars during their evolution, except for limited sources of specific isotopes (during the AGB stage and possibly from some novae). On the other side of the coin, they are produced in the ISM at a rate $r_\ell(t) \equiv \sum_{i,j} r_{i,j \rightarrow \ell}(t)$, therefore the abundance (by number) x_ℓ of the element ℓ is determined by the equation

$$\frac{d}{dt}(x_\ell M_g) = -x_\ell \psi + r_\ell M_g, \quad (11)$$

or, using equation (8), by the equation

$$M_g \frac{dx_\ell}{dt} = -x_\ell R \psi + r_\ell M_g. \quad (12)$$

To solve equation (12), it is necessary to evaluate the term $r_\ell(t)$, using equation (4). Following convention we assume that the normalized supernova rate is proportional to the SFR, $\xi(t) \equiv \psi_{\text{SM}}(t)/\psi_{\text{SN}}(t_{\text{Gal}}) = \psi(t)/\psi(t_{\text{Gal}})$, making no distinction between supernovae types I and II. This is a good approximation because the stars that end their life as SN II are high mass stars and then characterized by short lifetimes with respect to the age of the Galaxy. We only use supernovae to scale the production rate for cosmic rays, not for the overall metallicity of the gas (for which the two types are implicitly combined in the IRA coefficients). As we will describe in the next section, the distinction between SN types

is made explicitly in the fully nonlinear chemical evolution models. With our assumption $x_i^{\text{GCR}}(t) = x_i^{\text{ISM}}(t)$, the production coefficients r_ℓ for both direct and inverse processes scale linearly with the gas metallicity Z , since the abundance of p and α remains *nearly* constant with time. For fusion α – α reactions the production coefficient is practically independent on Z . Therefore, for *direct* p and α induced reactions and *inverse* CNO induced reactions, we obtain

$$r_\ell(t) = \xi(t) \frac{Z(t)}{Z(t_{\text{Gal}})} r_\ell(t_{\text{Gal}}) \equiv \frac{r_\ell(t_{\text{Gal}}) t_0}{M_0 Z(t_{\text{Gal}})} \psi(t) Z(t), \quad (13)$$

where we have defined a timescale $t_0 = M_0/\psi(t_{\text{Gal}})$. For ${}^6\text{Li}$ and ${}^7\text{Li}$ we must also include *fusion* α – α reactions,

$$r_\ell(t) = \xi(t) r_\ell(t_{\text{Gal}}) \equiv \frac{r_\ell(t_{\text{Gal}}) t_0}{M_0} \psi(t). \quad (14)$$

Although the same analytic expression describes both direct and inverse processes, keep in mind that under our assumptions the Z dependence in the first case represents the instantaneous interstellar abundances, while in the second case it is the GCR composition.

With these definitions, it is straightforward to solve equation (12) together with equation (8) and (9):

$$x_\ell(Z) = x_{\ell,\text{BB}} \exp\left(-\frac{R}{P_Z} Z\right) + \frac{r_\ell(t_{\text{Gal}}) t_0 P_Z}{(1-2R)^2 Z(t_{\text{Gal}})} \left[\exp\left(-\frac{R}{P_Z} Z\right) - \left(1 + \frac{1-2R}{P_Z} Z\right) \exp\left(-\frac{1-R}{P_Z} Z\right) \right], \quad (15)$$

for direct and inverse processes, and

$$x_\ell(Z) = x_{\ell,\text{BB}} \exp\left(-\frac{R}{P_Z} Z\right) + \frac{r_\ell(t_{\text{Gal}}) t_0}{1-2R} \left[\exp\left(-\frac{R}{P_Z} Z\right) - \exp\left(-\frac{1-R}{P_Z} Z\right) \right], \quad (16)$$

for fusion reactions. Any contribution from Big Bang nucleosynthesis is included as an initial abundance $x_{\ell,\text{BB}}$. Only for ${}^7\text{Li}$ the abundance depends on all of the processes we have discussed, including a significant cosmological contribution.

Equations (15) and (16) show that the light elements evolution is determined by the combination of stellar destruction, which reduces the initial Big Bang abundance, and cosmic-ray production that is proportional to $r_\ell(t_{\text{Gal}}) t_0$. Thus, according to the SM, all the physics of Galactic evolution is parameterized by the single quantity t_0 while the remaining quantities in equations (15) and (16) depend only on stellar properties.

In the absence of infall, the star formation rate must exponentially decrease with time since inert remnants inevitably result from stellar evolution. With this assumed rate, it is straightforward to solve eq. (8) and (9), obtaining

$$M_g(t) = M_0 e^{-t/\tau}, \quad (17)$$

$$\psi(t) = \frac{M_0}{(1-R)\tau} e^{-t/\tau}, \quad (18)$$

and

$$Z(t) = \frac{P_Z}{(1-R)\tau} t. \quad (19)$$

From eq. (19) we obtain $\tau \simeq 4.2$ Gyr by requiring that by $t = t_\odot = 8.5$ Gyr the metallicity has reached the solar value $Z_\odot = 0.02$. For $t_{\text{Gal}} \simeq 13$ Gyr, eq. (19) also gives $Z(t_{\text{Gal}}) \simeq 1.5Z_\odot$. Notice that Sandage (1986) estimated $\tau \simeq 4$ Gyr. Then for t_0 , we obtain

$$t_0 \equiv \frac{M_0}{\psi(t_{\text{Gal}})} = (1-R)\tau e^{t_{\text{Gal}}/\tau} \simeq 72 \text{ Gyr}. \quad (20)$$

The coefficients $r_\ell(t_{\text{Gal}})$ are given by eq. (4). The production coefficients $\mathcal{P}_{i,j \rightarrow \ell}$ and the trapping fractions $S_{i,j \rightarrow \ell}$ are given by Table 1 and 2, respectively. For both GCR and ISM at $t = t_{\text{Gal}}$ we have adopted a solar composition, $x_{\text{H}} = 0.91$, $x_{\text{He}} = 0.089$, $x_{\text{C}} = 3.30 \times 10^{-4}$, $x_{\text{N}} = 1.02 \times 10^{-4}$, and $x_{\text{O}} = 7.73 \times 10^{-4}$ (Grevesse & Sauval 1998). The values of $r_\ell(t_{\text{Gal}})$ obtained in this way are listed in Table 3. With these, and the value of t_0 given by eq. (20), we obtain the curves shown in Figures 1–4.

For Li evolution, shown in Figures 1 and 2, the predicted abundance remains very close to the primordial value, represented by the Spite plateau, up to $[\text{Fe}/\text{H}] \simeq -1.4$. At higher metallicities the predicted abundance increases about tenfold, although remaining significantly below the upper envelope of the observational data and the solar system meteoritic value. We will see in Section 4 that a more realistic model of Galactic evolution considerably reduces the predicted Li abundance at high metallicity, thus highlighting the need to include an additional (stellar) source of Li at later Galactic epochs. In Fig. 1, we see that the main contribution to the rise at $[\text{Fe}/\text{H}] \geq -2$ comes from fusion reactions that depend linearly on the relative fraction of GCR α particles. If, as reported in *e.g.* Meyer et al. (1998) and Wiebel-Sooth & Biermann (1999), these are depleted relative to CNO by as much as a factor of 5 without a change in spectrum, then the rise is delayed and the enrichment of Li reduced as displayed. The SM predictions for Be and B (Figures 3 and 4) produce reasonable fits to the observed abundances near $Z \simeq Z_\odot$, but fail at low metallicity. This is simply seen from equation (15) which, for $Z \ll Z_\odot$, gives the approximate behavior of the abundance of Be and B at low metallicity:

$$x_\ell(Z) \simeq \frac{1}{2} \frac{r_\ell(t_{\text{Gal}})t_0}{P_Z Z(t_{\text{Gal}})} Z^2, \quad (21)$$

showing a *quadratic* dependence on Z , at variance with the nearly linear trend up to $[\text{Fe}/\text{H}] \simeq -1.3$ (see Boesgaard et al. 1999) in the observational data. In contrast, Li ($=^6\text{Li}+^7\text{Li}$) is predicted to have a linear dependence with Z ,

$$x_{\text{Li}} \simeq x_{\text{Li,BB}} + \frac{r_{\text{Li}}(t_{\text{Gal}})t_0 - R x_{\text{Li,BB}}}{P_Z} Z \quad (22)$$

or,

$$\left(\frac{\text{Li}}{\text{H}}\right) \simeq \left(\frac{\text{Li}}{\text{H}}\right)_{\text{BB}} + k \left(\frac{Z}{Z_{\odot}}\right), \quad (23)$$

where

$$k \simeq \frac{r_{\text{Li}}(t_{\text{Gal}})t_0 Z_{\odot}}{x_{\text{H}} P_Z}, \quad (24)$$

and $r_{\text{Li}}(t_{\text{Gal}}) = r_6(t_{\text{Gal}}) + r_7(t_{\text{Gal}}) \simeq 9.8 \times 10^{-28} \text{ s}^{-1}$ for fusion reactions (see Table 3). In eq. (24) we have neglected the small effect of astration of primordial Li represented by the term $-R x_{7,\text{BB}}$ in eq. (23). The value of k has been determined observationally by Ryan et al. (2000) in a relatively small sample of carefully selected low metallicity stars (Ryan, Norris & Beers 1999). For a parametric linear fit they find $k = (1.1 \pm 0.7) \times 10^{-8}$. With $x_{\text{H}} = 0.91$ the SM with our parameters predicts $k \simeq 6.2 \times 10^{-9}$. This accordance indicates that the spallation scenario is likely correct, not that the closed box model is necessarily appropriate, because this expansion is correct only for near solar abundances and, as we have seen, the SM predictions are not consistent with each other. We therefore pass to the more complex model and show how the light element evolution can be better modeled, though at the expense of a considerably more complex treatment for the Galaxy.

4. Results for Light Element Evolution in a Multizone-Multi Population Framework for Galactic Chemical Evolution

We now consider the production of LiBeB nuclei in the framework of a more complex model of Galactic evolution. We recall briefly some important features of the model adopted (for a more detailed discussion see Ferrini et al. 1992, 1994). This multiphase and multi-zone model is able to follow the abundances of H, D, ^3He , ^4He , ^{12}C , ^{13}C , ^{14}N , ^{16}O , ^{20}Ne , ^{24}Mg , ^{28}Si , ^{32}S , ^{40}Ca , and ^{56}Fe and has recently been extended to s - and r -process elements (Travaglio et al. 1999). The model follows the interconnected evolution of three different regions in the Galaxy: halo, thick disk, and thin disk (*multizone* treatment). Relaxing the IRA takes into account detailed stellar nucleosynthesis as well as finite stellar lifetimes. The multiphase approach considers the different phases of the matter in the Galactic system: (i) stellar populations; (ii) stellar remnants; (iii) interstellar matter phases. A fundamental feature of the model is self-regulation through the internal processes that allow for the transformation of matter from one phase to another. These interactions produce the time dependence of the total mass fraction in each phase and the chemical abundances in the ISM and in stars. The star formation rate $\psi(t)$ is determined self-consistently by the interaction among the different phases of matter. This is very important because in the majority of the existing models, such as the SM described in Sec. 3, the formal time dependence for the SFR is

assumed *a priori*. The initial mass function adopted in this model is based on the analysis of Ferrini (1991) of the fragmentation of molecular clouds in the solar neighborhood, and is constant in space and time.

We have included the nucleosynthesis processes responsible for the evolution of LiBeB nuclei in this general Galactic model but we emphasize that *no other modification has been made to the model parameters or equations*. The results we report here require the input from our standard version that has been successfully used to analyze a number of Galactic evolution problems (see *e.g.* Shore & Ferrini 1995). The nonlinear evolution equations that determine the Li, Be and B abundances x_ℓ (by number), including spallation and fusion process, are:

$$\frac{dx_{\ell,H}}{dt} = r_{\ell,H} - x_{\ell,H} \frac{W_H}{g_H + c_H}, \quad (25)$$

$$\frac{dx_{\ell,T}}{dt} = r_{\ell,T} - x_{\ell,T} \frac{W_T}{g_T + c_T} + f_H(x_{\ell,H} - x_{\ell,T}) \frac{g_H}{g_T + c_T}, \quad (26)$$

$$\frac{dx_{\ell,D}}{dt} = r_{\ell,D} - x_{\ell,D} \frac{W_D}{g_D + c_D} + f_T(x_{\ell,T} - x_{\ell,D}) \frac{g_T}{g_D + c_D}, \quad (27)$$

where $\ell = {}^6\text{Li}, {}^7\text{Li}, {}^9\text{Be}, {}^{11}\text{B}$ is the light element under consideration. Here f_H and f_T are, respectively, the infall rates for gas flowing from the halo into the thick disk, and from thick disk into the thin disk: $f_H = 0.10$ and $f_T = 0.0065$ are the choices made for the solar neighborhood, that reproduce the mass ratio of the visible mass in the three zones. The quantities g_L and c_L are the gas and cloud fractions in the halo, thick disk, thin disk, respectively, where $L = H, T$, or D denotes the Galactic zone. The destruction terms in the three zones are represented by $W_L(t) = \sum_i W_{i,L}(t)$, where

$$W_{i,L}(t) = \sum_j \int_{m_{\min}}^{m_{\max}} \tilde{Q}_{ij}(m) X_j[t - \tau_Z(m)] \psi_L[t - \tau_Z(m)] dm, \quad (28)$$

is the mass fraction injected in the ISM as element i from stars ending their evolution at the time t . In order to compute the nucleosynthesis production of a star of mass m , the astration matrix $Q_{ij}(m)$ has been introduced, following Talbot & Arnett (1973). The $\{ij\}$ element of this matrix represents the fraction of the star mass initially in the form of chemical species j , transformed and ejected as chemical species i , $Q_{ij}(m) = m_{ij}^{\text{exp}}/m_j$. The quantity $\tilde{Q}_{ij}(m)$ is obtained weighting the contribution of the normal evolving stars, including stars exploding as SN II and the binary system ending as SN I. As we discussed in the previous section, for the closed box the two types have been combined for their contributions to cosmic ray production but the full chemical evolution model accounts for the distinctions between these two types of supernovae.

In Figures 2–4 we show the abundances predicted by our model, obtained following the nucleosynthesis prescriptions described in Section 2. The different trends for the metallicity as function of time contribute as well to the differences apparent as shown in Figure 5. In the multiphase model, Z is not a linear function of time. In fact, the IRA is relaxed and the consequences are particularly notable at low Z , when the finite stellar lifetime is most important. After $t \simeq 2$ Gyr, (or $\log Z \simeq -2.5$) the SM provides a good approximation of the numerical model. This is just the range, $[\text{Fe}/\text{H}] \geq -0.8$, where the abundances of LiBeB elements predicted by the two schemes are most similar. The displacement is essentially in $[\text{Fe}/\text{H}]$ for this reason.

Another important question for chemical evolution models is the normalization in the predicted abundances of LiBeB elements. It is common practice (see for example Prantzos et al. 1993; Fields & Olive 1999a,b; Vangioni-Flam & Cassé 1999) to normalize the final abundances of GCR-only isotopes ${}^6\text{Li}$, ${}^9\text{Be}$, ${}^{10}\text{B}$ to the observed abundances at $[\text{Fe}/\text{H}] = 0$. Consequently the GCR yields of ${}^7\text{Li}$ and ${}^{11}\text{B}$ are scaled by a factor that is the average of the three scaling factors of these isotopes. We stress that the results of our models, shown in Figures 2–4, are obtained without any *ad hoc* normalization. The most evident and relevant feature of the new curves is its improved agreement with the observations: whereas the simple model yields a quadratic dependence of $[\text{Be}/\text{H}]$ and $[\text{B}/\text{H}]$ with $[\text{Fe}/\text{H}]$, the multiphase Galactic evolution model more nearly approaches the observed approximately linear trend for increasing values of metallicity. Thus, the slope for the abundance of Be and B vs. $[\text{Fe}/\text{H}]$ is ~ 2 for the halo, ~ 1.4 for the thick disk, ~ 0.7 for the thin disk. For comparison, Boesgaard et al. (1999) determined empirically for Be vs. $[\text{Fe}/\text{H}]$ a best-fit slope ~ 1 – 1.3 for $-3.0 < [\text{Fe}/\text{H}] < -1$, and ~ 0.6 – 0.7 for $-1.0 < [\text{Fe}/\text{H}] < 0.1$. It worth stressing this result because it is different from the conclusions obtained previously by other authors (see for example Vangioni-Flam & Cassé 1999; Fields & Olive 1999a). Even treating only the direct processes (i.e. the “GCR standard” as named in Vangioni-Flam & Cassé 1999), it is possible to reproduce quite well the observed trend of Be and B with $[\text{Fe}/\text{H}]$. From this trial we can conclude that in our scenario of Galactic evolution the “GCR standard” does not lead to a quadratic dependence of Be and B vs Fe, in contrast to, for example, Vangioni-Flam & Cassé (1999) and Fields & Olive (1999a).

The model reaches the solar photospheric B abundance $\log(\text{B}/\text{H}) = -9.45$ (Grevesse & Sauval 1998) at $[\text{Fe}/\text{H}] = 0$, whereas it exceeds the solar Be abundance $\log(\text{Be}/\text{H}) = -10.85$ (Chmielewski, Müller, & Brault 1975). This trend also appears in other published results (see *e.g.* Lemoine et al. 1998) that overproduce Be relative to its meteoritic and photospheric values. This discrepancy with the observed Be and B abundances at higher metallicity may be partially due to stellar depletion. The systematic departures at more recent times of the numerical predictions from the observations suggests this interpretation. In Table 4 we

compare the model results at solar metallicity with the solar system data (Hanon et al. 1999). We remind the reader that the model results refer to ISM abundances, whereas spectroscopic observations can only provide stellar photospheric values. A comparison of the theoretical curves and the Be abundance at the time of formation to the Solar System (meteoritic value) and in the ISM would represent a more appropriate test of the model. Although the ISM value 4.6 Gyr ago is unknown, Howk et al. (2000) provide a lower limit on the *contemporary* interstellar $\log B/H > -9.60$. If we assume that this is the same difference as between the models and the stellar observations, there are two possible explanations. The more radical is that there could be indications of a mixing mechanism – presently unexplained – for stars younger than about 1 to 2 Gyr. This is based on the metallicity at which the first systematic deviations appear in the Be and B evolution models. We re-iterate that the models have not been normalized nor have any parameters used for the stellar population and heavy metal evolution been altered to obtain agreements between the observed and predicted light element abundances. We favor a more prosaic explanation: that the Be and B abundances have been systematically *underestimated* for the higher metallicity stars, likely due the combined effects of NLTE and the “missing opacity” problem most recently outlined by Bell et al. (2001) and references therein. If so, assuming the appropriateness of our embedded assumptions about the production rates, the models point to the systematic correction that is needed and could also serve as a constraint in the search for the responsible opacity sources *without the need to invoke new production sources for the light elements at late times in galactic history*.

Direct processes and the fusion reaction do not reproduce the observed values for ${}^7\text{Li}$ at high $[\text{Fe}/\text{H}]$. This is similar to the results of the SM and also to those obtained in the literature. It is well known that the case of ${}^7\text{Li}$ is more complex: lithium is not a GCR-only element and stellar production cannot be ignored (see *e.g.* Travaglio et al. 2001). For ${}^{11}\text{B}/{}^{10}\text{B}$, the models predict an essentially constant ratio, 2.4, from spallation processes alone. A possible solution is the production of ${}^{11}\text{B}$ by ν -induced spallation of ${}^{12}\text{C}$ in SN II (Woosley & Weaver 1995) but this and other likely contributing sources have not been included in the calculation. From Figures 2–4, we note a decrease of the slope of the the halo and thick disk curves at low $[\text{Fe}/\text{H}]$ in the cases of Be and B. This is in better agreement with the observational data in this range than the results obtained including only direct processes. The contribution of inverse processes is more significant at low metallicity, because during the first evolutionary phases of the Galaxy the abundance of interstellar CNO target nuclei is very low. For Li, the contribution of inverse processes is marginal with respect to the pre-Galactic Big Bang production.

5. Discussion and Conclusions

The SM is a closed box model with IRA that provides a useful test for more complex models of Galactic evolution because its predicted metallicity is the highest possible. This is due to the approximate treatment (IRA) of gas return, which maximizes metal production from stars and the efficiency of its re-incorporation into stars, and to the absence of gas dilution by infall. Therefore, in the usual abundance vs. $[\text{Fe}/\text{H}]$ plots, SM predictions roughly determine the right boundary of the region occupied by more complex models for which these assumptions are relaxed; our multiphase model of Galactic evolution relaxes the IRA approximation and allows infall of gas allowing us to follow simultaneously the evolution of three Galactic zones (halo, thick disk and thin disk). This fact is evident from the comparison of the results of the SM with those of our model shown in Figures 2, 3 and 4. For the halo component, the two models give similar results. This is because the halo behaves like a closed box, even though it loses gas to form the thick disk. Here the loss of gas is not what matters but the fact that there is *no feedback* on the halo from the other Galactic zones. Thus, the LiBeB isotope productions in the halo follow the prediction of the SM but are shifted to lowest values of $[\text{Fe}/\text{H}]$ because the IRA overestimates the actual metal production. The slope of $\log(\text{Be}/\text{H})$ and $\log(\text{B}/\text{H})$ vs. $[\text{Fe}/\text{H}]$ for the halo is close to 2, the value for the SM. Indeed, this quadratic dependence of the abundance of these elements on metallicity in the halo is a natural consequence of our halo picture.

On the other hand, for the thick and thin disk, the IRA is not the only difference with the SM and the couplings halo–thick disk, and thick disk–thin disk play important roles which are, of course, ignored in closed box models. Thus, in addition to an overall rightward shift of the abundances vs. $[\text{Fe}/\text{H}]$ with respect to the SM the fact that the thick disk receives chemically enriched gas from the halo, and the thick disk from the thick disk, allows progressively shallower slopes of the abundance curves vs. $[\text{Fe}/\text{H}]$. Our goal here is not much to discriminate among different stellar populations in the Galaxy. Rather, we deliberately loosely use the terms “halo”, “thick disk” and “thin disk” to describe coupled Galactic zones forming in sequential cascade, and we emphasize the different behavior of such a complex system with respect to a homogeneous one-zone model, no matter how sophisticated.

An additional complication in the interpretation of the results is the customary (but unavoidable) way of plotting the abundance of chemical species not as function of time, as they are calculated, but as function of metallicity Z or $[\text{Fe}/\text{H}]$, to allow a comparison with spectroscopic data. Whereas time and metallicity scale linearly in the case of the SM and the use of either variable is equivalent, the same is not true for our multiphase model. First, the relation of metallicity with time is not linear. Second, each Galactic zone follows a different enrichment history. For example, during the first 3 Gyr of Galactic life (where $[\text{Fe}/\text{H}]$ rises

from minus infinity up to about -0.7) the abundance of LiBeB elements is higher in the halo, followed by the thick disk and the thin disk. This simply reflects the behavior of the star formation rates in the three zones (see Fig. 5 of Pardi et al. 1995); for the same reason, $[\text{Fe}/\text{H}]$ follows the same ordering (see also their Fig. 6), so that a given value of $[\text{Fe}/\text{H}]$ is reached first by the halo and later on by the thick disk and the thin disk. Since LiBeB abundances grow more rapidly than Fe with time, however, their ordering in the abundance vs. $[\text{Fe}/\text{H}]$ plot is reversed. At a specified value of $[\text{Fe}/\text{H}]$, the halo has the lowest abundance, and the thin disk has the highest. These facts should be kept in mind when interpreting our results for LiBeB shown in Fig. 2–4.

In conclusion, we show that the multi-zone multi-population model we used previously for other aspects of Galactic evolution produces quite good agreement with the *linear* trend observed at low metallicities as consequences of multi-zone coupling of a galactic chemical evolution model and detailed accounting for the feedback between phases without the instantaneous recycling approximation or time dependent variations in the cosmic-ray spectrum or the initial mass function. No *special* mechanisms are needed to produce the increase in abundances at late times in Galactic history (*e.g.* novae producing excess Li, variations in the low energy part of the cosmic ray spectrum, etc.). Indeed, the *overproduction* of the light elements in our calculations suggests that the abundances of these elements derived from stellar photospheric observations may be *underestimates*. We argue that reported discrepancies between theory and observations do not represent a nucleosynthetic problem, but instead are the consequences of inaccurate treatments of Galactic evolution.

We are grateful to Sam Austin for cross section data in advance of publication and to Constantine Deliyannis, Brian Fields, Peter Biermann, and the late Reuven Ramaty for discussions and correspondence. SNS was supported in part by NASA and thanks the Osservatorio Astrofisico di Arcetri and the director, Franco Pacini, for their kind invitations for several extended summer visits in 2000–2001. FF, DG, and SNS acknowledge support from the Italian Ministry for the University and for Scientific and Technological Research (MURST) through a COFIN-2000 grant. We thank the (anonymous) referee for helpful questions, especially those to which we openly respond in the final section of this paper.

REFERENCES

- Bell, R. A., Balachandran, S. C., and Bautista, M. 2001, *ApJ*, 546, L65
- Balachandran, S. 1990, *ApJ*, 354, 310
- Bonifacio, P., & Molaro, P. 1997, *MNRAS*, 285, 847
- Boesgaard, A. M., Deliyannis, C. P., King, J. R. Ryan, S. G., Vogt, S. S., & Beers, T. C. 1999, *AJ*, 117, 1549
- Cesarsky, C. L. 1980, *ARA&A*, 18, 289
- Chen, Y. Q., Nissen, P. E., Benoni, T., Zhao, G. (2001) *A&A*, 371, 943
- Chmielewski, Y., Brault, J. W., & Müller, E. A. 1975, *A&A*, 42, 37
- Cunha, K., Smith, V. V., Boesgaard, A. M., & Lambert, D. L. 2000, *ApJ*, 530, 939
- Dodds, D., Wolfendale, A. W., & Wdowczyk, J. 1976, *MNRAS*, 176, 345
- Duncan, D. K., Primas, F., Rebull, L. M., Boesgaard, A. M., Deliyannis, C. P., Hobbs, L. M., King, J. R., & Ryan, S. G. 1997, *ApJ*, 488, 338
- Duncan, D. K., Peterson, R., Thorburn, J. A., & Pinsonneault, M. H. 1998, *ApJ*, 499, 871
- Ferrini, F. 1991, in “Chemical and Dynamical Evolution of Galaxies”, eds. F. Ferrini, F. Matteucci, & J. Franco, (Pisa: ETS), 511
- Ferrini, F., Matteucci, F., Pardi, M. C., & Penco, U. 1992, *ApJ*, 387, 138
- Ferrini, F., Mollà, M., Pardi, M. C., & Diaz, A. 1994, *ApJ*, 427, 745
- Fields, B. D., & Olive, K. A. 1999, *ApJ*, 516, 797
- Fields, B. D., & Olive, K. A. 1999, *New Astr.*, 4, 255
- Fields, B. D., & Olive, K. A., Vangioni-Flam, E., Cassé, M. 2000, *ApJ*, 540, 930
- Fulbright, J. P. 2000, *AJ*, 120, 1841
- Galli, D., Palla, F., Ferrini, F., & Penco, U. 1995, *ApJ*, 443, 536
- García López, R. J., Lambert, D. L., Edvardsson, B., Gustafsson, B., Kiselman, D., & Rebolo, R. 1998, *ApJ*, 500, 241

- Gloecker, G., & Jokipii, J. R. 1967, *ApJ*, 299, 745
- Goldstein, M. L., Fisk, L. A., & Ramaty, R. 1970, *Phys. Rev. Lett.*, 25, 12
- Grevesse, N. & Sauval, A. J. 1998, *SSR*, 85, 161
in “Cosmic Abundances”, eds. S.S. Holt & G. Sonneborn, A.S.P. Conference Series,
p. 117
- Hanon, P., Chaussidon, M., & Robert, F. 1999, *MPS*, 34, 247
- Howk, J. C., Sembach, K. R., & Savage, B. D. 2000, *ApJ*, 543, 278
- Ip, W. H., & Axford, W. I. 1985, *A&A*, 149, 7
- Lemoine, M., Ferlet, R., Vidal-Madjar, A., Emerich, C., & Bertin, P., 1993, *A&A*, 269, 469
- Lemoine, M., Vangioni-Flam, E., & Cassé, M. 1998, *ApJ*, 499, 735
- Mercer, D. J., Austin, S. M., Brown, J. A., Danczyk, S. A., Hirzebruch, S. E., Kelley, J. H.,
Suomijärvi, T., Roberts, D. A., & Walker, T. P. 2001, *Phys. Rev. C*, 63, 065805
- Meneguzzi, M., Audouze, J., & Reeves, H. 1971, *A&A*, 15, 337
- Meyer, J.-P., Drury, L. O’C., & Ellison, D. C. 1998, *Space Sci. Rev.*, 86, 179
- Mitler, H. E. 1972, *Ap&SS*, 17, 186
- Pardi, M.C., Ferrini, F., & Matteucci, F. 1995, *ApJ*, 444, 207
- Prantzos, N., Cassé, M., & Vangioni-Flam, E. 1993, *ApJ*, 403, 630
- Prantzos, N., Tosi, M., & von Steiger, R. (eds.) 1998, “Primordial Nuclei and their Galactic
Evolution”, *Space Science Reviews* 84, Kluwer Academic Publishers
- Primas, F., Duncan, D. K., Peterson, R. C., & Thorburn, J. A. 1999, *A&A*, 343, 545
- Primas, F., Molaro, P., Bonifacio, P., & Hill, V. 2000a, *A&A*, 362, 666
- Primas, F., Asplund, M., Nissen, P. E., & Hill, V. 2000b, *A&A*, 364, L42
- Ramaty, R., Vangioni-Flam, E., Cassé, M., & Olive, K. 1999, *PASP*, 111, 651
- Read, S.M., & Viola, V.E. Jr. 1984, *Atomic data and nuclear data tables*, 31, 359
- Reeves, H., & Meyer, J.-P. 1978, *ApJ*, 226, 613

- Ryan, S. G., Norris, J. E., & Beers, T. C. 1999, *ApJ*, 523, 654
- Ryan, S. G., Beers, T. C., Olive, K. A., Fields, B. D., Norris, J. E. *ApJ*, 530, L57
- Sandage, A. 1986, *A&A*, 161, 89
- Shore, S. N., & Ferrini, F. 1995, *Fund. of Cosm. Phys.*, 16, 1
- Spite, F. & Pallavicini, R. (eds.) 1995, “Stellar and Interstellar Lithium and Primordial Nucleosynthesis”, *Mem. Soc. Astron. It.*, vol. 66
- Talbot, R.J., & Arnett, W.D. 1973, *ApJ*, 186, 51
- Tinsley, B. M. 1980, *Fund. of Cosm. Phys.*, 5, 287
- Travaglio, C., Galli, D., Gallino, R., Busso, M., Ferrini, F., & Straniero, O. 1999, *ApJ*, 521, 691
- Travaglio, C., Randich, S., Galli, D., Lattanzio, J., Elliott, L. M., & Ferrini, F. 2001, *ApJ*, in press
- Vangioni-Flam, E., & Cassé, M. 1999, in “Galaxy Evolution: connecting the distant Universe with the local fossil record”, eds. M. Spite and F. Crifo (Paris: Editions Frontières)
- Vangioni-Flam, E., Ramaty, R., Olive, K.A., & Cassé, M. 1998, *A&A*, 337, 714
- Vangioni-Flam, E., Cassé, M., & Audouze, J. 2000, *Phys. Rep.*, 333, 365
- Yoshii, Y., Kajino, T., & Ryan, S. G. 1997, *ApJ*, 485, 605
- Webber, W. R. 1998, *ApJ*, 506, 329
- Wiebel-Sooth, B., & Biermann, P. L. 1999, in *Landolt-Börnstein*, vol. VI/2 Supplement (Berlin: Springer-Verlag)
- Woosley, S. E., & Weaver, T. A. 1995, *ApJS*, 101, 181

Table 1. TRAPPING FRACTIONS $S_{i,j \rightarrow \ell}$

i	j	ℓ	$S_{i,j \rightarrow \ell}$
p	C,N,O	${}^6,{}^7\text{Li}, {}^9\text{Be}, {}^{10,11}\text{B}$	1
α	C,N,O	${}^6,{}^7\text{Li}, {}^9\text{Be}, {}^{10,11}\text{B}$	0.86
α	α	${}^6,{}^7\text{Li}$	0.46
C,N,O	p, α	${}^6,{}^7\text{Li}, {}^9\text{Be}, {}^{10,11}\text{B}$	0.25

Table 2. PRODUCTION COEFFICIENTS $\mathcal{P}_{i,j \rightarrow \ell}$ (IN 10^{-25} s^{-1})

i, j or j, i	${}^6\text{Li}$	${}^7\text{Li}$	${}^9\text{Be}$	${}^{10}\text{B}$	${}^{11}\text{B}$
p, C	2.64	4.82	0.723	5.00	13.3
p, N	4.21	2.52	1.08	2.94	5.93
p, O	3.03	4.75	0.957	3.15	6.91
α, C	11.5	15.2	3.84	13.0	24.1
α, N	4.17	4.80	1.83	9.26	15.2
α, O	3.93	5.11	1.86	0.87	11.2
α, α	0.74	1.94			

Table 3. PRODUCTION RATES $r_{i,j \rightarrow \ell}(t_{\text{Gal}})$ FOR THE CLOSED-BOX MODEL (IN 10^{-30} s^{-1})

i, j	${}^6\text{Li}$	${}^7\text{Li}$	${}^9\text{Be}$	${}^{10}\text{B}$	${}^{11}\text{B}$
direct processes					
p, C	79.3	145	21.7	150	399
p, N	39.0	23.3	10.0	27.2	55.0
p, O	213	334	67.3	222	486
total p, CNO	331	502	99.0	399	940
α, C	29.0	38.4	9.70	32.8	60.9
α, N	3.26	3.75	1.43	7.23	11.9
α, O	23.2	30.2	11.0	5.15	66.3
total α, CNO	55.5	72.4	22.1	45.2	139
α, α	270	707			
inverse processes					
C, p	19.8	36.2	5.43	37.5	99.9
N, p	9.77	5.85	2.51	6.82	13.8
O, p	53.3	83.5	16.8	55.4	122
total CNO, p	82.9	126	24.7	99.7	236
C, α	8.44	11.2	2.82	9.54	17.7
N, α	0.94	1.09	0.42	2.10	3.45
O, α	6.76	8.79	3.20	1.50	19.3
total CNO, α	16.1	21.1	6.44	13.1	40.5

Table 4. SOLAR SYSTEM AND ISM LiBeB VALUES COMPARED TO MODEL

Value	$(^6\text{Li} + ^7\text{Li})/\text{H}$	$^9\text{Be}/\text{H}$	$(^{10}\text{B} + ^{11}\text{B})/\text{H}$
Chondrites ^(a)	5.1×10^{-10}	2.1×10^{-11}	3.3×10^{-10}
Orgueil ^(a)	2.0×10^{-9}	2.6×10^{-11}	7.6×10^{-10}
Solar Photosphere ^(b)	1.3×10^{-11}	1.4×10^{-11}	3.5×10^{-10}
ISM	$> 3.7 \times 10^{-10}$ ^(c)	...	$> 2.5 \times 10^{-10}$ ^(d)
Model: $[\text{Fe}/\text{H}]=0$	1.1×10^{-9}	6.0×10^{-11}	5.3×10^{-10}

References. — ^(a) Hanon et al. (1999), ^(b) Grevesse & Sauval (1998),
^(c) Lemoine et al. (1993), ^(d) Howk et al. (2000)

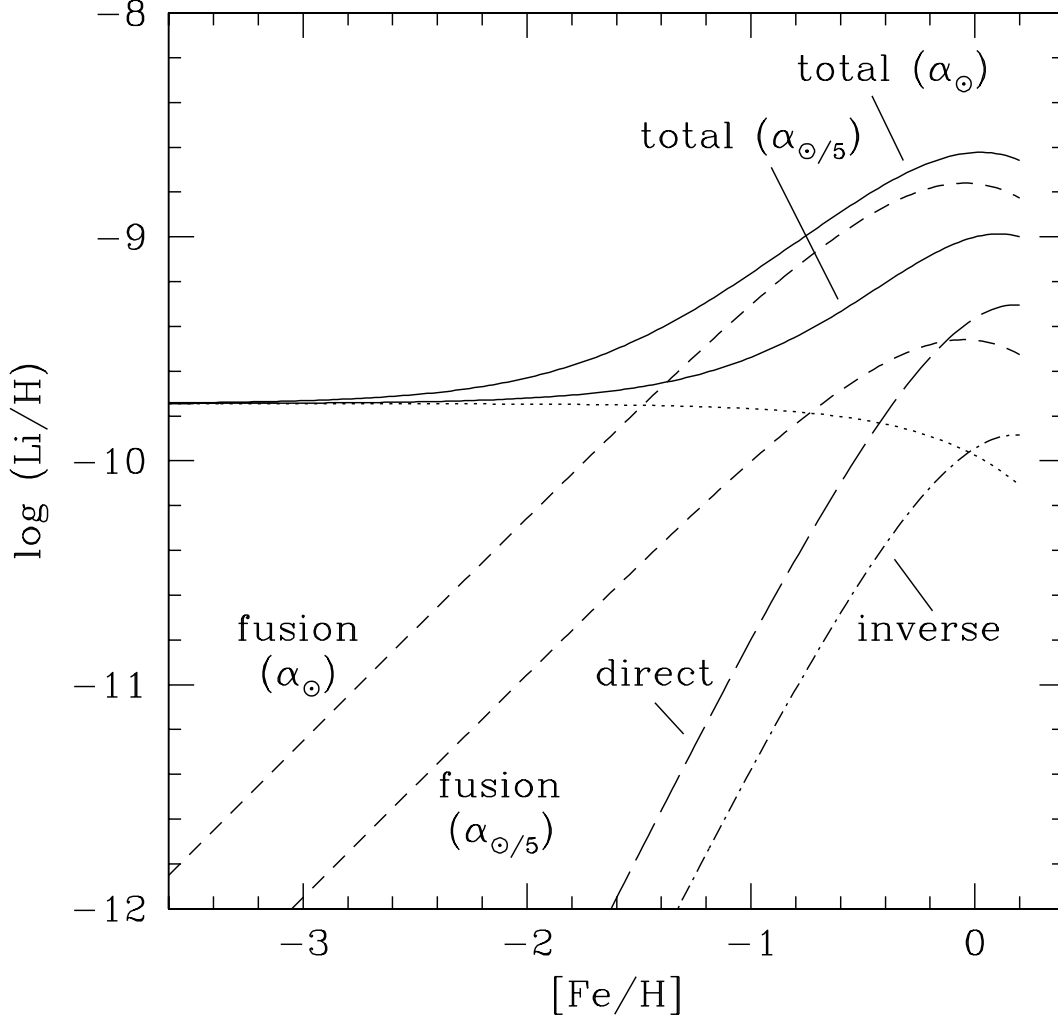


Fig. 1.— Contributing physical processes to Li evolution ($=^6\text{Li}+^7\text{Li}$) according to the closed box model. *Dotted line*: Big Bang nucleosynthesis and stellar astration; *short-dashed line*: fusion α – α reactions; *long-dashed line*: direct processes; *dash-dotted line*: inverse processes. The upper most curve shows the result obtained with a standard (solar) GCR composition as described in Sect. 3, the lower curve employed a reduced α contribution in the GCR flux by a factor of 5 (see text).

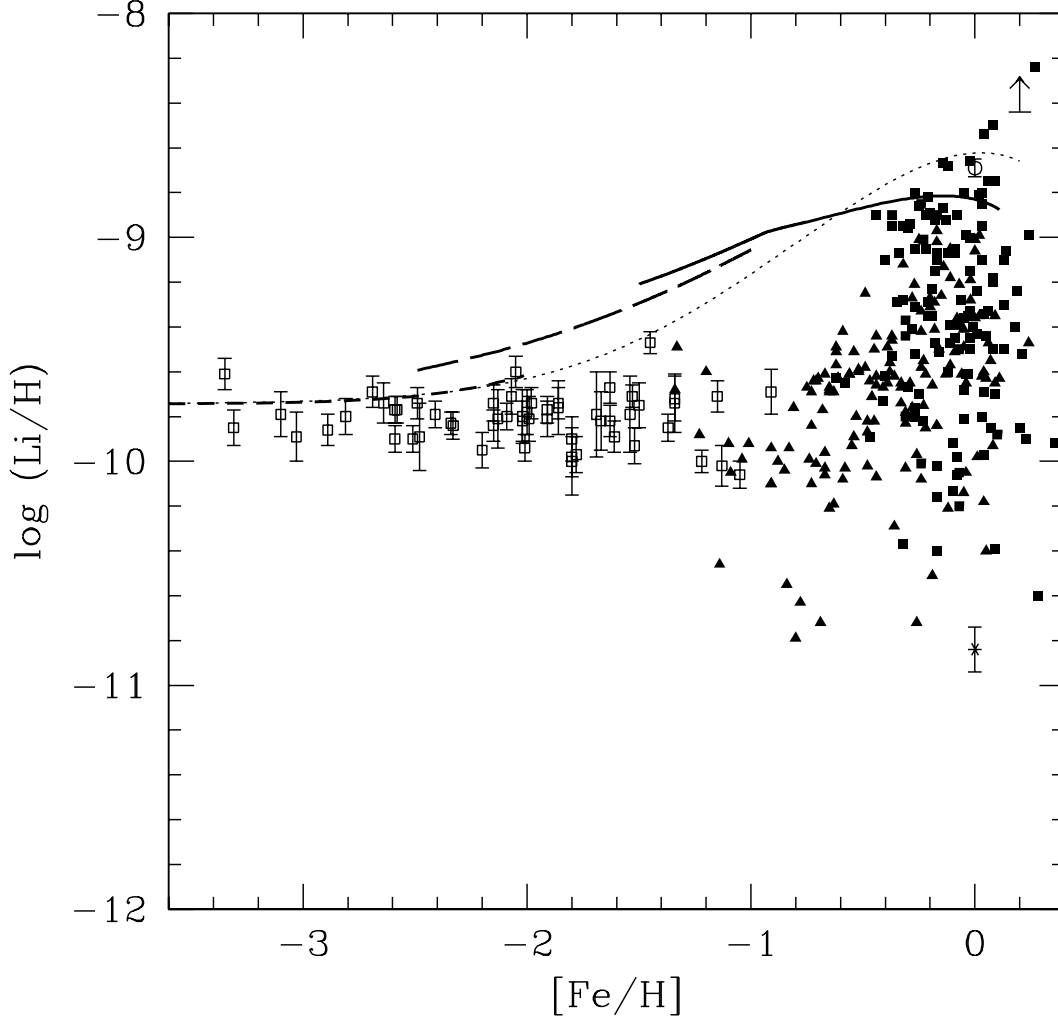


Fig. 2.— Evolution of Li ($=^6\text{Li}+^7\text{Li}$) according to the closed box model (*thin dotted line*) and our numerical model (*thick short-dashed line*, halo; *thick long-dashed line*, thick disk; *thick solid line*, disk) including the contribution of fusion, direct and inverse reactions. The meteoritic and the solar photospheric Li abundances (from Grevesse & Sauval 1998) are indicated by an *open circle* and an *asterisk*, respectively. The lower limit on the ISM abundance of Li determined by Lemoine et al. (1993) has been placed at $[\text{Fe}/\text{H}] = 0.2$. Stellar photospheric data are from Bonifacio & Molaro (1997) (*open squares*), Balachandran (1990) (*filled squares*), Fulbright (2000) (*filled circles*), and Chen et al. (2001) (*filled triangles*).

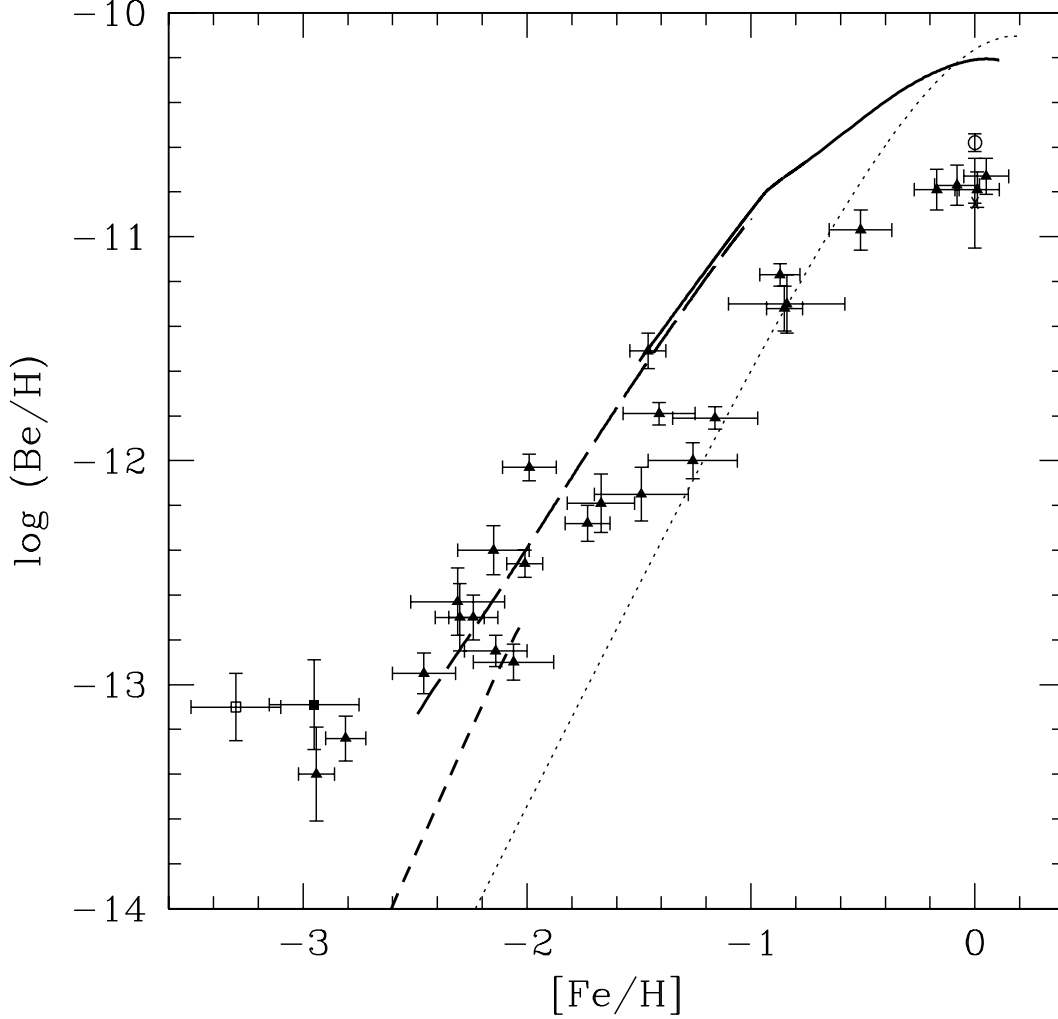


Fig. 3.— Evolution of ${}^9\text{Be}$ according to the closed box model (*thin dotted line*) and our numerical model (*thick short-dashed line*, halo; *thick long-dashed line*, thick disk; *thick solid line*, disk) including the contribution of direct and inverse reactions. The meteoritic (from Grevesse & Sauval 1998) and the solar photospheric (from Chmielewski, Müller, & Brault 1975) ${}^9\text{Be}$ abundances are indicated by an *open circle* and an *asterisk*, respectively. Stellar photospheric data are from Boesgaard et al. (1999) (*filled triangles*), Primas et al. (2000a) (G64-12, *open square*), and Primas et al. (2000b) (LP815-43, *filled square*).

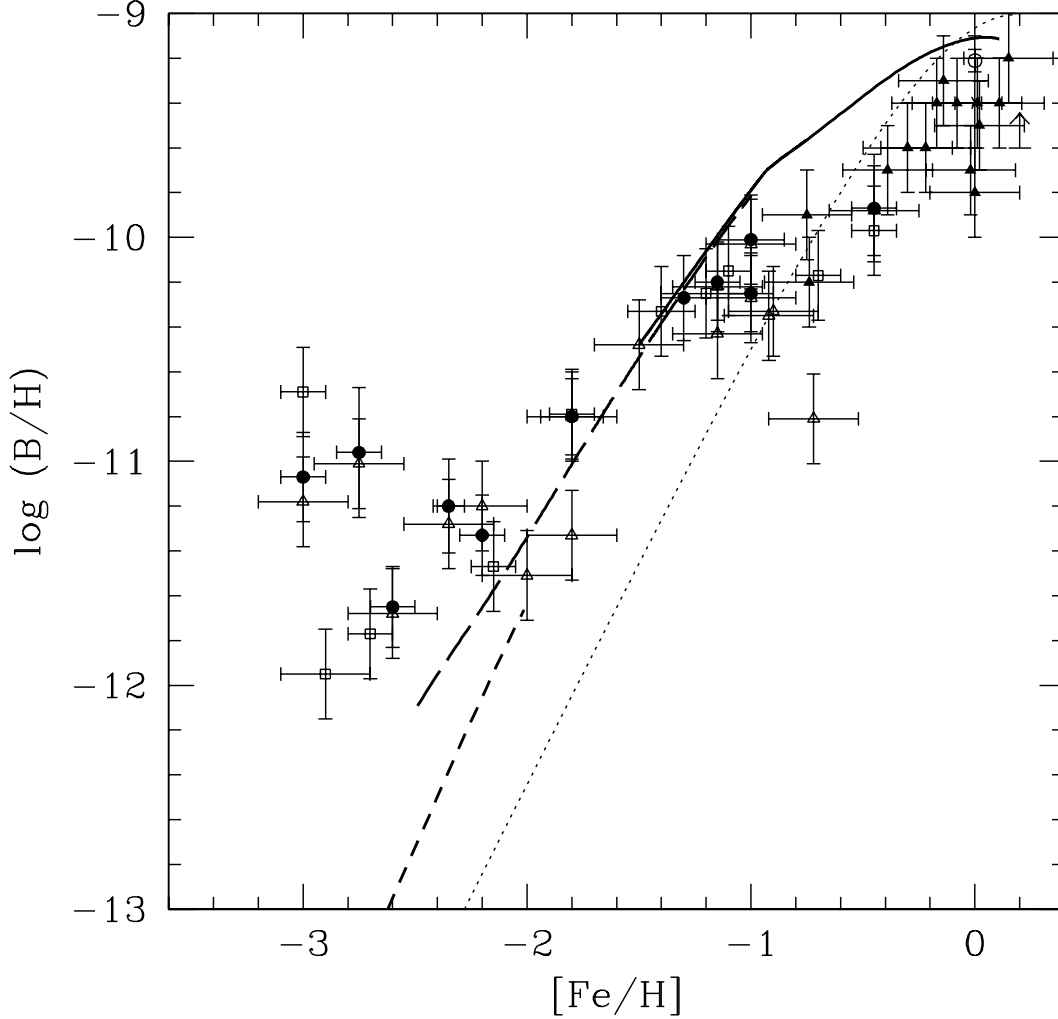


Fig. 4.— Evolution of B ($=^{10}\text{B}+^{11}\text{B}$) according to the closed box model (*thin dotted line*) and our numerical model (*thick short-dashed line*, halo; *thick long-dashed line*, thick disk; *thick solid line*, disk) including the contribution of direct and inverse reactions. The meteoritic and the solar photospheric B abundances (from Grevesse & Sauval 1998) are indicated by an *open circle* and an *asterisk*, respectively. The lower limit on the ISM abundance of B determined by Howk et al. (2000) has been placed at $[\text{Fe}/\text{H}] = 0.2$. Stellar photospheric data are from Cunha et al. (2000) (*filled squares*), Primas et al. (1999) (*open triangles*), Duncan et al. (1997) (*filled circles*), and García López et al. (1998) (*empty squares*).

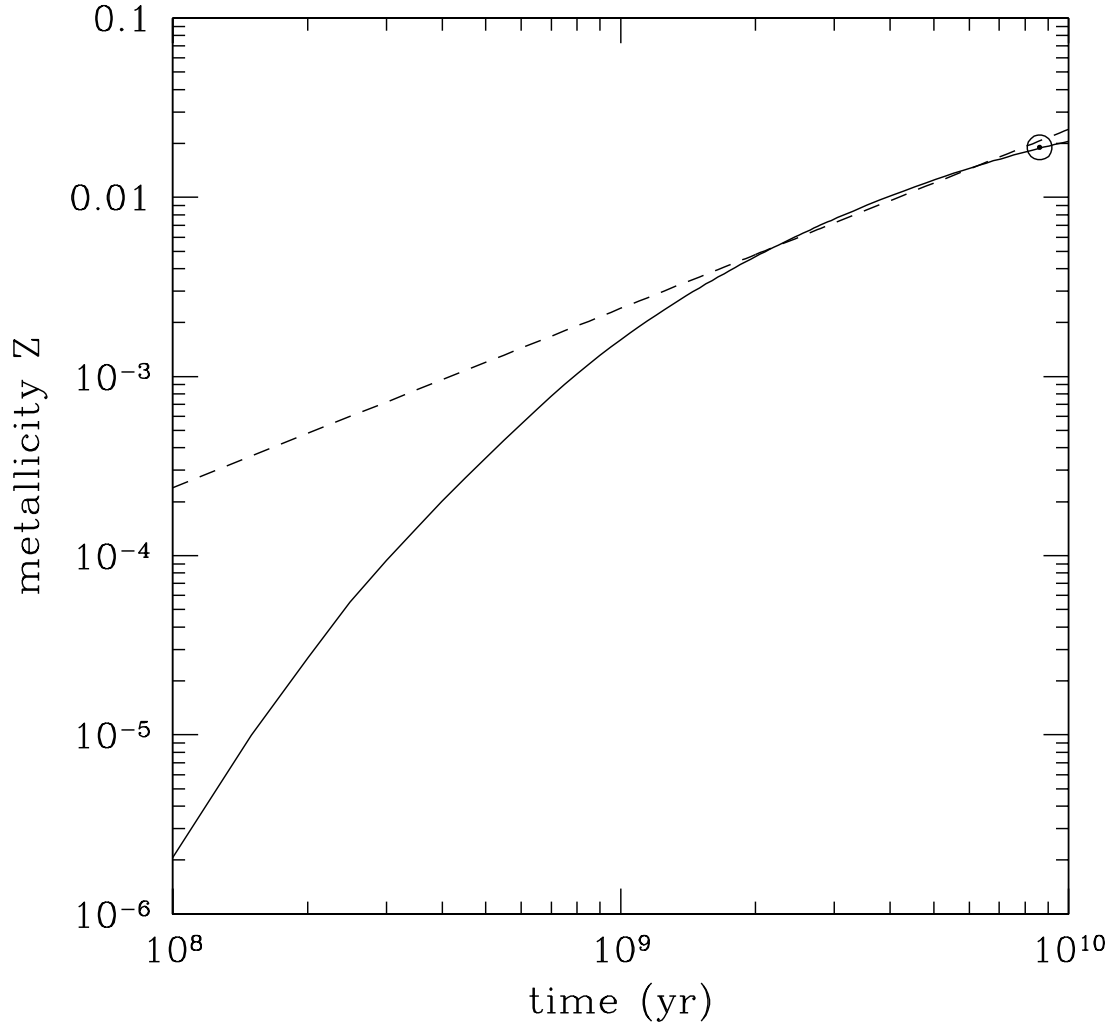


Fig. 5.— Comparison of the metallicity Z predicted by the SM (*dashed line*) and by our model (*solid line*) as function of time. The solar symbol indicates the solar metallicity at the epoch of formation of the Sun, $t = 8.5$ Gyr, assumed in our model.